Fabrication of PVDF/HMO Mixed Matrix Membrane: Effect of HMO Loading on Oil/Water Separation

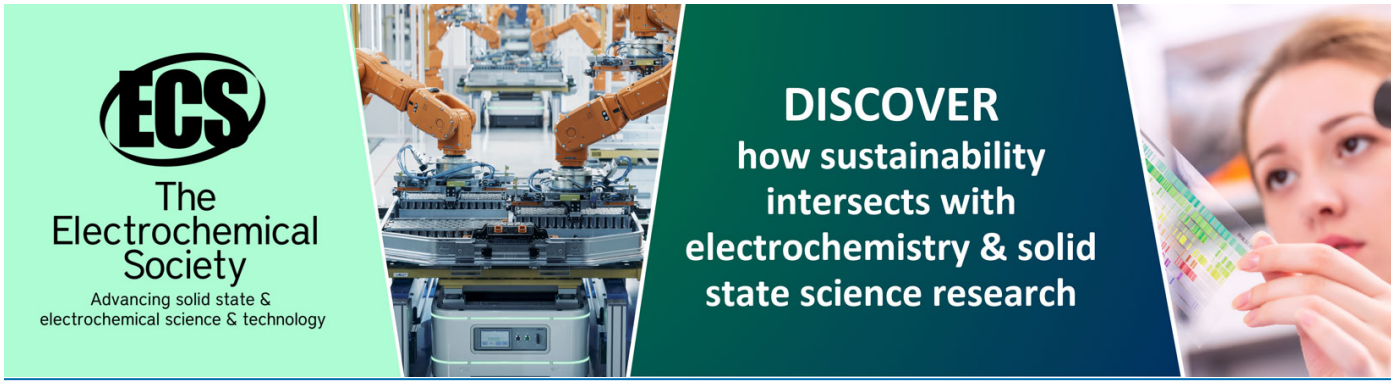

IOP Conf. Series: Materials Science and Engineering **736** (2020) 052004 doi:10.1088/1757-899X/736/5/052004

Fabrication of PVDF/HMO Mixed Matrix Membrane: Effect of HMO Loading on Oil/Water Separation

N. H. Ismail,[1, 2] W. N. W. Salleh,[1, 2]* H. Hasbullah,[1, 2] F. Aziz,[1, 2] N. A. Awang,[1, 2] S. Z. N. Ahmad,[1, 2] N. Rosman,[1, 2] A.F. Ismail [1, 2]

[1] Advanced Membrane Technology Research Centre (AMTEC), Universiti Teknologi Malaysia, Skudai, Johor Bahru, Malaysia.
[2] School of Chemical and Energy Engineering, Faculty of Engineering, Universiti Teknologi Malaysia, Skudai, Johor Bahru, Malaysia.
Correspongin author's email: hayati@petroleum.utm.my

Abstract. In this research, polyvinylidene fluoride (PVDF) polymer was mixed with hydrous manganese oxide (HMO) nanoparticles to form a mixed matrix membrane (MMM) with excellent wetting properties to separate oil/water emulsion. Accordingly, the effects of different HMO loading (3, 5, 7 and 10 wt%) on the membrane's water flux and oil rejection performance were studied. The characteristics of the MMM were demonstrated via scanning electron microscopy (SEM), atomic force microscopy (AFM), as well as water and oil contact angle analysis. The HMO nanoparticles, which has large amounts of hydroxyl (-OH) groups, enhanced the membrane's hydrophilicity. The fabricated MMM became hydrophilic and underwater oleophobic with the presence of -OH groups on the membrane surface. Specifically, the MMM surface repelled the oil droplets and had high affinity towards the water molecules, thereby demonstrating good oil/water separation performance. PVDF/HMO with 10 wt% of HMO had the highest water flux (402 L/m^2.h) and oil rejection rate (93%).

1.0 Introduction

Researchers have long attempted to find ways to rectify oil spills as well as domestic and industrial discharges. Extensive treatment methods have been extensively developed to at least alleviate the oily wastewater problem owing to its contribution to the environmental pollution that endangers living things so as human health. Floatation, coagulation, and biological treatment are among the most commonly-used conventional treatment methods [2]. Unstable oil/ water emulsions or free-floating oil can be easily removed by these conventional separation processes. However, it is almost impossible for the aforementioned conventional methods to separate oil molecules from stable oil/ water emulsions. As the oil droplets in stable oil/ water emulsions require a long time to float or coagulate, chemicals are unable to break the emulsions effectively [3].

Under these circumstances, membrane technology is a promising method to solve the oily wastewater problem. This is especially true for membranes whose pore sizes (in the micrometer to nanometer range) are smaller than those of oil droplets (> 20 μm) [4]. Evidently, the factors that prevent the polymeric membrane from being the best method to separate oil/ water emulsions are hydrophobicity and fouling. Thus, polymeric membranes have been modified by means of (i) the addition of additional polymers or inorganic nanoparticles to the host polymer (polymer blending), or (ii) modifications of the surfaces of the polymeric membranes (i.e. surface modification). The purpose of modification is to increase the membrane's hydrophilicity since hydrophobic membranes lead to fouling issue [5].

Inorganic materials are among the most common polymeric membrane-modification techniques in the treatment of oily wastewater. When inorganic materials are mixed with polymeric solutions, a mixed matrix membrane (MMM) will be obtained. Numerous researchers have compared the water flux and oil rejection capacities of MMMs and neat polymers, whereupon it was discovered that MMM performed three to five times better than unmodified polymers [6-9]. Apparently, the addition of these additives not only enhanced the membrane wetting property; it also modified the surface roughness and increased the porosity of the membrane, eventually giving rise to high water flux and oil rejection rate.

Liu et al. [10] have fabricated MMMs from the mixture of an inorganic nanoparticle – silica oxide (SiO2) – with chitosan (host polymer) and glutaraldehyde (GA). Subsequently, the solution was coated on polyvinyldene fluoride (PVDF) membranes. It has been reported that SiO2 had a sufficient number of oxygen molecules in a mole to increase the surface hydrophilicity of the membrane [11]. Furthermore, the MMM coat on the PVDF membrane increased its surface roughness owing to the reaction between SiO2 and the hydroxyl groups of chitosan. As it turned out, the reaction between the inorganic nanoparticles and host polymer altered the membrane's wetting properties. Specifically, the membrane became more hydrophilic when the water contact angle changed from 120 ± 1° to ~0°, and more oleophobic as the oil contact angle increased from 2 ± 1° to 151 ± 1°.

Meanwhile, the amount of loaded nanoparticles is also a crucial determinant of water flux and oil rejection. Ahmad et al. [12] have studied the effect of bentonite nanoclay loading on polyvinyl chloride (PVC) membranes in the production of ultrafiltration (UF) MMMs. The objective of introducing the bentonite nanoclay to the PVC matrix was to ensure that the fabricated membrane offered good resistance to oily wastewater. Accordingly, the MMM which contained 6 wt% of bentonite nanoclay had highest water flux (186 L/m2·h) and oil rejection rate (97%). Also, the addition of this inorganic nanoparticle also increased membrane surface roughness, porosity, pore density, and hydrophilicity (from ~75° to ~57°).

In this study, PVDF was used as the host polymer. It was impregnated with hydrous manganese oxide (HMO), and the effects of the loading of the mixture on the membrane's water flux and oil rejection performances were evaluated. HMO was the additive of choice owing to its abundance of hydroxyl (-OH) groups that could increase the hydrophilicity of the membrane [6]. The HMO was self-synthesized via oxidation of permanganate by referring to Parida et al. [14] methods. On another note, the morphology, surface roughness (Ra), and wetting properties of the membrane are further discussed in subsequent section. The relationship between the aforementioned characteristics and membrane performance (i.e. water flux and oil rejection capacity) were investigated as well.

2.0 Materials and Methods

2.1 Materials

Polyvinylidene fluoride (PVDF, Kynar @ 760) pellets (Arkema Inc., Philadelphia, USA) were the main polymer. Meanwhile, manganese (II) sulfate monohydrate ($MnSO_4.H_2O$), potassium permanganate ($KMnO_4$), and sodium hydroxide (NaOH) by Merck were used to synthesize the HMO nanoparticles. The solvent was N-Methyl-2-Pyrrolidone (NMP) (Merck, > 99%), while glycerol (Merck, > 99.5%) was utilized post-treatment without further purification.

2.2 Synthesis of HMO nanoparticles

Permanganate was generated via the oxidation of manganese ions as per the method of HMO synthesis by Parida et al. [14]. Solution 1 – potassium permanganate ($KMnO_4$) – was dissolved in deionized water, following which 1 M of sodium hydroxide (NaOH) was added until the pH become 12.5. At the same time, manganese (II) sulfate monohydrate ($MnSO4.H_2O$) was dissolved in deionized water to form solution 2. Subsequently, solution 1 was added drop-wise to Solution 2 under vigorous stirring to give rise to a brown precipitate (HMO). The HMO was washed with DI water until it became neutral (pH 7). After that, the HMO powder was left for several weeks for aging purpose. Finally, the synthesized HMO

nanoparticles were dried in vacuum oven at 65°C for 24 h, after which they were ground, sieved, and stored in a desiccator prior to use.

2.3 Polymeric Dope Solution Preparation

To fabricate the MMM, 3 wt% of HMO was added to solution that contained 18 wt% of PVDF and NMP. To avoid precipitation, the additive was gradually added to the solution. Next, the solution was stirred at 400 rpm for 24 h at 60°C until a homogenous solution was obtained. The dope solution was placed in a sonicator to remove the bubbles formed during stirring. The same procedure was repeated with different amounts of HMO-loadings (i.e. 5, 7, and 10 wt%). Meanwhile, a pristine PVDF membrane was prepared exactly using the same method, albeit in the absence of HMO nanoparticles. The nomenclatures of the resultant MMMs were assigned with respect to the form of PVDF of the pristine membrane and the amount of HMO utilized in the PVDF/HMO-loading (i.e. PVDF/HMO_3, PVDF/HMO_5, PVDF/HMO_7, and PVDF/HMO_10).

2.4 Membrane Fabrication

Some 20 mL of dope solution was poured onto a smooth and clean glass plate to generate a flat sheet membrane. The solution was cast at a speed of 5 cm/s and membrane thickness 250 – 300 μm using a roller glass. The flat sheet membrane on the glass plate was immersed in tap water for phase inversion. The delaminated membrane then was transferred to another coagulation bath. To ensure the complete removal of all residues, the membrane was immersed in the coagulation bath for 3 days. The membrane was then subjected to post-treatment using glycerol prior to drying in an oven at 40°C for 24 h. Each differently-loaded membrane was tested using three different samples, and three readings were taken for each sample.

2.5 Characterization

The surface morphology of the membrane was inspected using a scanning electron microscope (SEM; model JEOL JSM-5610LV). Atomic force microscope (AFM) images were scanned at a resolution of 10 μm × 10 μm to determine the surface roughness of the membrane, or mean surface roughness (R_a). RO water and recycle engine oil were used as the probe liquid for the water contact angle and oil contact angle goniometers respectively (OCA 15Pro, DataPhysics). The surface roughness of the membrane was studied using a tapping-mode AFM (model NX-Hivac). Accordingly, membrane porosity was measured as per Eq. 1 using the gravimetric method.

$$\varepsilon = \frac{\omega_1 - \omega_2}{A \times l \times d_w} \tag{1}$$

where ω_1 was the weight of the wet membrane, ω_2 weight of the dry membrane, A membrane effective area (m^2), d_w water density (0.998 g/cm^3), and l membrane thickness (m). The membrane was immersed in deionized water for 1 min, after which it was weighed. Subsequently, the membrane was dried until its weight was consistent.

In addition, with the utilization of water permeability and porosity data, the Guerout–Elford–Ferry equation was employed to evaluate the mean pore radius (r_m) of the membrane, as stated in Eq. 2:

$$r_m = \sqrt{\frac{(2.9 - 1.75\varepsilon) \times 8\eta l Q}{\varepsilon \times A \times \Delta P}} \tag{2}$$

where η was the water viscosity (8.9×10^{-4} Pa·s), Q volume of the permeate pure water per unit time (m^3/s), and ΔP operative pressure (0.5 MPa). The membranes were vacuum-dried 100°C for 24 h. In the water uptake analysis, the membranes were weighed and immersed in deionized water at room

temperature for another 24 h. Then, the wet membranes were wiped dry and immediately reweighed. Eq. 3 below shows the water uptake analysis, in wt%:

$$Water \quad uptake = \frac{W_{wet} - W_{dry}}{W_{dry}} \times 100 \tag{3}$$

where W_{wet} and W_{dry} were the weights of the wet and dry membranes respectively.

A cross-flow membrane system was employed to determine the membrane's pure water flux. Prior to flux determination, all membranes were compacted at 2 bar for 30 min until a steady-state condition was achieved. Subsequently, the equation below was used to calculate the pure water flux of the membrane (J_w, L/m^2·h) at a ambient pressure of 1 bar:

$$Jw = Q/(A\times \Delta T) \tag{4}$$

where Q was the quantity of permeate (L), A effective membrane surface area (m^2), and ΔT sampling time (h). Additionally, Eq. 4 was employed to calculate the permeate flux during the treatment of the synthetic oily solution. The membrane oil rejection rate (R) was determined as per Eq. (5). The efficacy of the membranes' separation of oil molecules from the oil-in-water emulsion was calculated using the equation below:

$$R = \left(1 - \frac{C_p}{C_f} \times 100 \right) \tag{5}$$

where R was the process of rejection ultrafiltration (%), C_p concentration of the permeate (%), and C_f concentration of the feed (%). A UV–vis spectrophotometer (DR5000, Hach) was used to determine the oil concentrations in the feed and permeate samples at a wavelength of 305 nm.

3.0 Results and Discussion

3.*1 Membrane surface morphology*

Figure 1 shows the upper surface of the membrane of the pristine PVDF membrane and PVDF/HMO for different amounts of HMO loading. Apart from being rougher and denser than other PVDF/HMO MMMs, the surface of the pristine PVDF contained glycerol which reduced the PVDF shrinkage problem. The presence of HMO in the PVDF/HMO MMM helped reduce the surface roughness relative to that of the pristine membrane, as proven by AFM (Section 3.2). Based on the SEM images, HMO was well-distributed on the surface of the membrane as there was no evidence of clear nanoparticle agglomeration. Evidently, surface roughness – which was an important determinant of membrane hydrophilicity – could also be proved by SEM, and will be further discussed in terms of AFM characterization. Increasing the HMO loading on the PVDF membrane matrix resulted in a smooth upper surface as shown in Table 1. This phenomenon was due to the presence of –OH groups on the surface of the membrane, which increased the water flux [15]. Moreover, the addition of HMO in the membrane solely generated Mn atoms on the surface as well. The existence of Mn on the PVDF/HMO MMM had high affinity for water molecules [16]. Accordingly, more water molecules were driven through the membrane, giving rise to a high water flux.

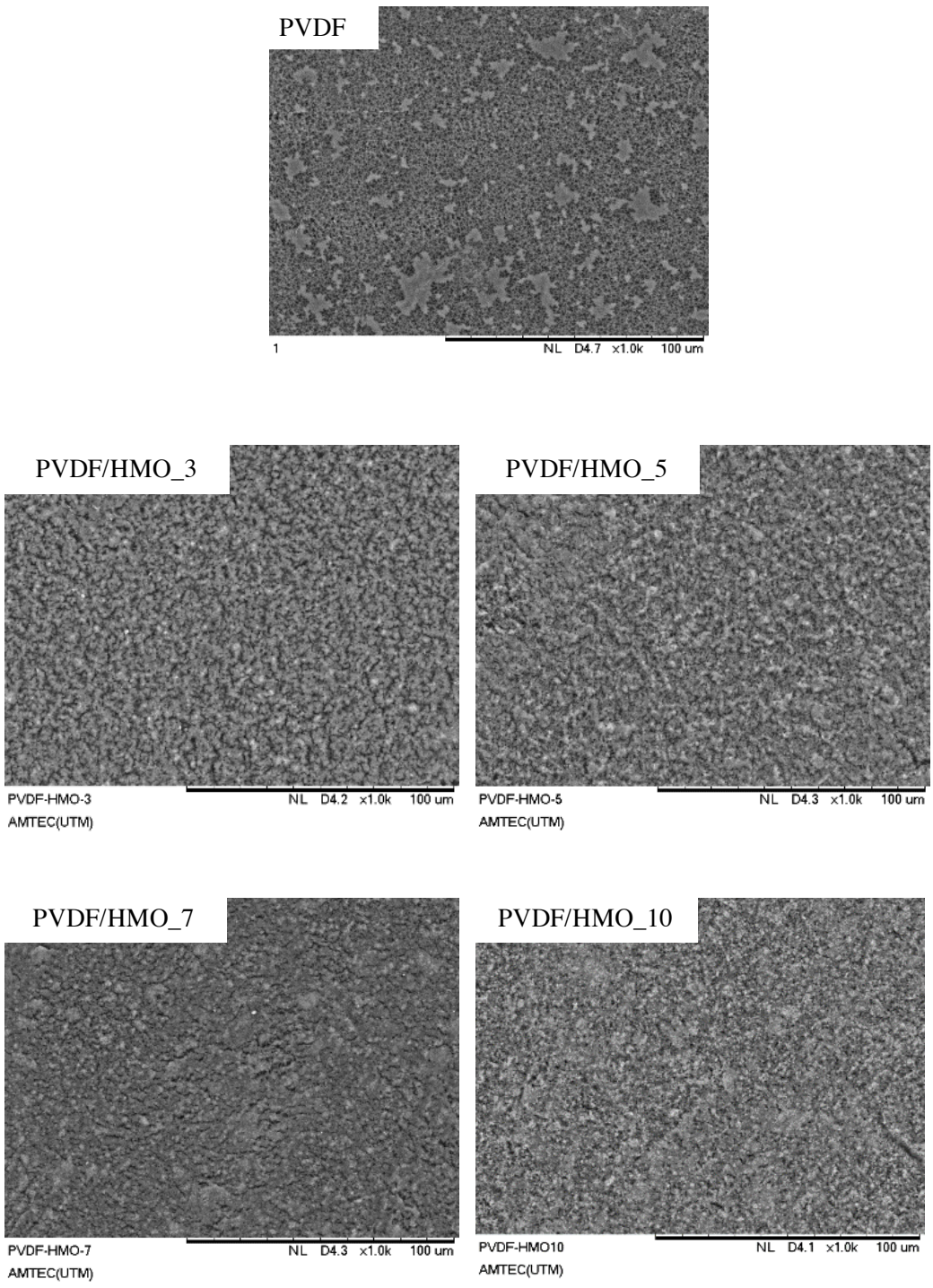

Figure 1: SEM images of pristine PVDF membrane and PVDF/HMO MMM top surface view

3.2 Membrane surface roughness

The surface roughness of the membrane was observed using the AFM. Apparently, surface roughness determines the membrane's wetting properties; high surface roughness translates into high membrane water flux [17]. However, high surface roughness may increase the membrane's susceptibility to fouling.

Accordingly, some of the researchers have modified the surfaces of membranes to reduce their roughness [18]. Based on the AFM results (Table 1), the pristine PVDF membrane had a higher surface roughness (R_a = 192 nm) as compared to the PVDF/HMO MMM. The addition of HMO to the PVDF matrix membrane reduced its surface roughness. Meanwhile, further increments in the HMO loading reduced the surface roughness from 178 to 119 nm. This was also proven by SEM characterization, in that the HMO impregnated membrane surface appeared to be smoother than the pristine PVDF. Nevertheless, a HMO loading of 10 wt% yielded greater surface roughness as that of 7 wt%, possibly due to the agglomeration of small amounts HMO that were not obviously seen on the membrane surface. However, with respect to these two membranes, the difference in surface roughness was less than 10%, so a significant effect on membrane performance was unlikely. The lower surface roughness of PVDF/HMO might also contribute to an increase in water flux [19]. Further effects of surface roughness will be discussed in terms of membrane water flux and oil rejection performance. Figure 2 shows the surface roughness of the pristine PVDF and PVDF/HMO_7.

Table 1: Pristine PVDF and PVDF/HMO membrane mean surface roughness (R_a) value

Membrane	PVDF	PVDF/HMO_3	PVDF/HMO_5	PVDF/HMO_7	PVDF/HMO_10
Surface roughness (R_a) (nm)	192	178	154	119	129

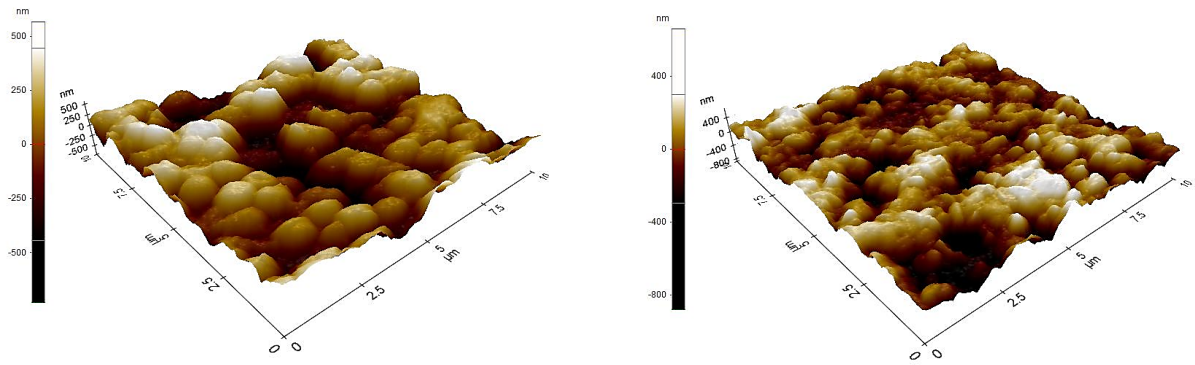

PVDF PVDF/HMO_7

Figure 2: Pristine PVDF and PVDF/HMO_7 membrane mean surface roughness (R_a)

3.3 Membrane surface wetting property

In the treatment of oily wastewater, membrane wetting is the most crucial factor for the generation of high water flux and oil rejection performance. Highly hydrophilic and oleophobic membranes are advantageous for this application. Table 2 shows the water and oil contact angles of pristine PVDF and PVDF/HMO MMM. PVDF is a naturally-hydrophobic material; in this study, the water contact angle of the pristine PVDF membrane was 99.3°. In addition, the oil contact angle was 0°, where the oil droplets immediately penetrated the membrane when they were dropped onto the surface of the PVDF membrane. This showed that the hydrophobic membrane had a high tendency to be fouled. At the same time, the oil droplets easily spread over the membrane's pores, resulting in pore blockage [20]. On the other hand, the addition of HMO to PVDF/HMO MMM reduced the water contact angle and increased the oil contact angle, thereby showing that the –OH groups and Mn atoms on the membrane surface resulted in higher hydrophilicity and oleophobicity vis-a-vis the pristine PVDF membrane. Ergo, the

effects of HMO loading on the two wetting properties of PVDF/HMO were clearly shown. This proved the abundant presence of –OH groups on the PVDF membrane matrix when a greater amount of HMO was used.

Table 2: Water and oil contact angle of pristine PVDF and PVDF/HMO membrane top surface

	Water contact angle (°)	Oil contact angle (°)
PVDF	99.3	0
PVDF/HMO_3	84.5	6.8
PVDF/HMO_5	72.3	17.0
PVDF/HMO_7	61.7	24.4
PVDF/HMO_10	58.7	35.1

3.4 Water Flux and Oil Rejection

Generally, to obtain high water flux and oil rejection performance, the membrane should be hydrophilic and oleophobic. Figure 3 shows the water fluxes and oil rejection performances of the pristine PVDF and PVDF/HMO membranes when an oily feed solution of concentration 500 ppm was used. The pristine PVDF membrane had a lower water flux (42 $L/m^2 \cdot h$) than the MMM. The addition of HMO to the PVDF/HMO membrane increased the water flux by almost 10 times (PVDF/HMO_10) relative to that of the pristine PVDF membrane. The presence of HMO attracted large amounts of –OH groups to the surface of the membrane [6]. In turn, the -OH groups did not only increase the hydrophilicity of the membrane; they also reduced the membrane's surface roughness. As high surface roughness membrane is prone to fouling, the addition of HMO reduces the surface roughness and generates high water flux. To elaborate, both aforementioned characteristics – wetting properties and surface roughness – are the drivers of high water flux [18].
The oil rejection performance of the pristine PVDF (94%) was slightly higher compared to that of the PVDF/HMO membrane (93.0 – 93.9%). Nevertheless, all fabricated membranes in this study were comparable with the performance of the present membrane. In addition, the pristine membrane was unable to withstand long operations owing to its oleophilicity, which allowed oil droplets to form a layer cake on the surface of the membrane, eventually resulting in pore blockage and hence, led to fouling [20].

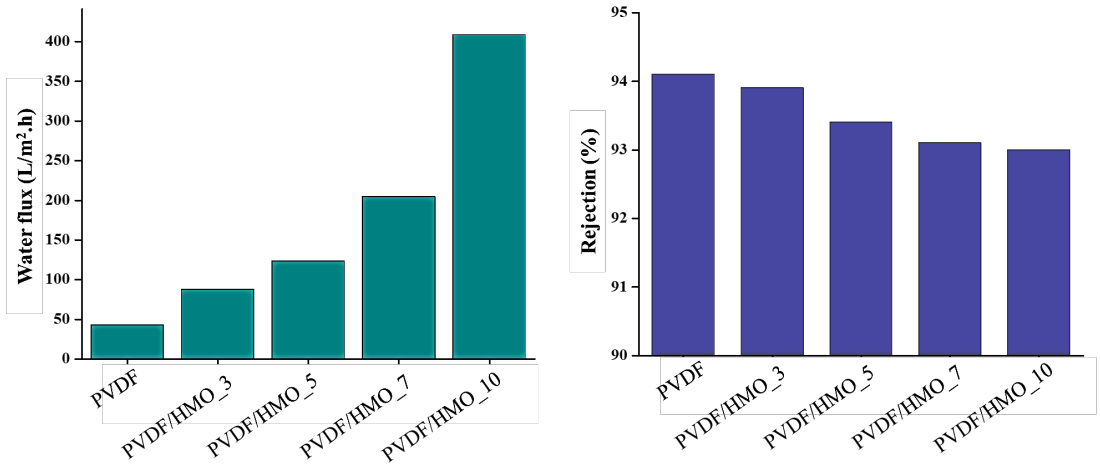

Figure 3: Pristine PVDF and PVDF/HMO membrane (a) water flux and (b) oil rejection at oily concentration of 500 ppm

4.0 Conclusion

Various amounts of HMO loading have been successfully incorporated into the PVDF/HMO MMM. The presence of HMO in the MMM reduced the membrane's surface roughness, thereby resulting in high water flux. PVDF/HMO_10 (which had 10 wt% of HMO) exhibited the highest water flux (402 L/m^2·h), which was almost 10 times that of the pristine PVDF membrane (42 L/m^2·h). The addition of HMO to the PVDF matrix membrane attracted large amounts of –OH groups and Mn atoms to the surface of the membrane, both of which reduced the water contact angle. The membrane hydrophilicity was increased almost 50% from pristine membrane (99.3°) with the existence of HMO in the PVDF matrix membrane (56.7°). In addition, HMO caused the surface of the membrane to be more repellence towards oil droplets, as proven by the oil contact angle. All fabricated membrane had oil rejection performances of more than 93%.

Acknowledgements
The authors would like to thank the Ministry of Education and Universiti Teknologi Malaysia for the financial support provided under MRUN-RU Partner Translational Research Program (Project Number: R.J1300000.7851.4L863) and Transdisciplinary Research (TDR) Grant (Project Number: Q.J130000.3551.05G76) in completing this work. N.H. Ismail would like to acknowledge the support from Universiti Teknologi Malaysia for ZAMALAH scholarship.

References

[1] Salahi A, Mohammadi T, Behbahani R M and Hemmati M 2015 Asymmetric polyethersulfone ultrafiltration membranes for oily wastewater treatment: synthesis, characterization, ANFIS modeling, and performance *J. Environ.Chem. Eng.* **3** 170.
[2] Yu L, Han M and He F 2017 A review of treating oily wastewater *Arab. J. Chem.* **10** S1913.
[3] Chakrabarty B, Ghoshal A K and Purkait M K 2008 Ultrafiltration of stable oil-in-water

emulsion by polysulfone membrane *J. Membr. Sci.* **325** 427.
[4] Deng Y, Zhang G, Bai R, Shen S, Zhou X and Wyman I 2019 Fabrication of superhydrophilic and underwater superoleophobic membranes via an in situ crosslinking blend strategy for highly efficient oil/water emulsion separation *J. Membr. Sci.* **569** 60.
[5] Sun W, Liu J, Chu H and Dong B 2013 Pretreatment and membrane hydrophilic modification to reduce membrane fouling *Membr.* **3** 226.
[6] Lai G, Yusob M, Lau W J, Gohari R J, Emadzadeh D, Ismail A F, Goh P S, Isloor A and Arzhandi M R D 2017 Novel mixed matrix membranes incorporated with dual-nanofillers for enhanced oil-water separation *Sep. Purif. Technol.* **178** 113.
[7] Ong C S, Lau W J, Goh P S, Ng B C and Ismail A F 2015 Preparation and characterization of PVDF–PVP–TiO_2 composite hollow fiber membranes for oily wastewater treatment using submerged membrane system *Desalin. Water Treat.* **53** 1213.
[8] Cao J, Cheng Z, Kang L, Chu M, Wu D, Li M, Xie S and Wen R 2017 Novel stellate poly(vinylidene fluoride)/polyethersulfone microsphere-nanofiber electrospun membrane with special wettability for oil/water separation *Mater. Lett.* **207** 190.
[9] Cui J, Zhou Z, Xie A, Wang Q, Liu S, Lang J, Li C, Yan Y and Dai J 2019 Facile preparation of grass-like structured NiCo-LDH/PVDF composite membrane for efficient oil–water emulsion separation *J. Membr. Sci* **573** 226.
[10] Liu C T, Su P K, Hu C C, Lai J Y and Liu Y L 2018 Surface modification of porous substrates for oil/water separation using crosslinkable polybenzoxazine as an agent *J J. Membr. Sci* **546** 100.
[11] Kusworo T D and Utomo D P 2017 Performance evaluation of double stage process using nano hybrid PES/SiO2-PES membrane and PES/ZnO-PES membranes for oily waste water treatment to clean water *J. Enviro. Chem. Eng.* **5** 6077.
[12] Ahmad T, Guria C and Mandal A 2018 Synthesis, characterization and performance studies of mixed-matrix poly (vinyl chloride)-bentonite ultrafiltration membrane for the treatment of saline oily wastewater *Process Saf. and Environ. Prot.* **116** 703.
[13] Yuan T, Meng J, Hao T, Wang Z and Zhang Y 2015 A Scalable Method toward Superhydrophilic and Underwater Superoleophobic PVDF Membranes for Effective Oil/Water Emulsion Separation *ACS Appl. Mater*. **7** 14896
[14] Parida K, Kanungo S and Sant B 1981 Studies on MnO2—I. Chemical composition, microstructure and other characteristics of some synthetic MnO_2 of various crystalline modifications *Electrochim. Acta* **26** 435.
[15] Gohari R J, Lau W J, Matsuura T and Ismail A F 2013 Effect of surface pattern formation on membrane fouling and its control in phase inversion process *J. Membr. Sci* **446** 326.
[16] Murray J W 1974 The surface chemistry of hydrous manganese dioxide *J. Colloid Interface Sci.* **46** 357.
[17] Ikhsan S N W, Yusof N, Aziz F, Misdan N, Ismail A F, Lau W J, Jaafar J, Salleh W N W, and Hairom N H H 2018 Efficient separation of oily wastewater using polyethersulfone mixed matrix membrane incorporated with halloysite nanotube-hydrous ferric oxide nanoparticle *Sep. Purif. Technol.* **199** 161.
[18] Islam M S, McCutcheon J R and Rahaman M S 2017 A high flux polyvinyl acetate-coated electrospun nylon 6/SiO_2 composite microfiltration membrane for the separation of oil-in-water emulsion with improved antifouling performance *J. Membr. Sci* **537** 297.
[19] Gohari R J, Halakoo E, Nazri N, Lau W J, Matsuura T, and Ismail A F 2014 Improving performance and antifouling capability of PES UF membranes via blending with highly hydrophilic hydrous manganese dioxide nanoparticles *Desalin.* **335** 87.
[20] Huang S, Ras R H A and Tian X 2018 Antifouling membranes for oily wastewater treatment: Interplay between wetting and membrane fouling *Curr. Opin. Colloid Interface Sci.* **36** 90.